Cellular nonmuscle myosins NMHC-IIA and NMHC-IIB and vertebrate heart looping

ARTICLE *in* DEVELOPMENTAL DYNAMICS · DECEMBER 2008

Impact Factor: 2.38 · DOI: 10.1002/dvdy.21645 · Source: PubMed

SPECIAL ISSUE RESEARCH ARTICLE

Cellular Nonmuscle Myosins NMHC-IIA and NMHC-IIB and Vertebrate Heart Looping

Wenge Lu,[1] Steven H. Seeholzer,[2,†] Mingda Han,[1] Anne-Sophie Arnold,[1] Maria Serrano,[1] Barbara Garita,[1] Nancy J. Philp,[3] Cassandra Farthing,[4,‡] Peter Steele,[5] Jizhen Chen,[1] and Kersti K. Linask[1]*

Flectin, a protein previously described to be expressed in a left-dominant manner in the embryonic chick heart during looping, is a member of the nonmuscle myosin II (NMHC-II) protein class. During looping, both NMHC-IIA and NMHC-IIB are expressed in the mouse heart on embryonic day 9.5. The patterns of localization of NMHC-IIB, rather than NMHC-IIA in the mouse looping heart and in neural crest cells, are equivalent to what we reported previously for flectin. Expression of full-length human NMHC-IIA and -IIB in 10 T1/2 cells demonstrated that flectin antibody recognizes both isoforms. Electron microscopy revealed that flectin antibody localizes in short cardiomyocyte cell processes extending from the basal layer of the cardiomyocytes into the cardiac jelly. Flectin antibody also recognizes stress fibrils in the cardiac jelly in the mouse and chick heart; while NMHC-IIB antibody does not. Abnormally looping hearts of the Nodal$^{\Delta\ 600}$ homozygous mouse embryos show decreased NMHC-IIB expression on both the mRNA and protein levels. These results document the characterization of flectin and extend the importance of NMHC-II and the cytoskeletal actomyosin complex to the mammalian heart and cardiac looping. *Developmental Dynamics 237:3577–3590, 2008.* © 2008 Wiley-Liss, Inc.

Key words: nonmuscle myosin; NMHC-IIA; NMHC-IIB; heart looping; cytoskeleton; flectin; nodal; asymmetry

Accepted 2 June 2008

INTRODUCTION

Previous observations established that the asymmetric, left-dominant, expression of a protein that we termed flectin within the myocardium and adjacent region of the cardiac jelly is important in heart looping. In the bilateral heart fields of the Hamburger and Hamilton (HH) stage 8 avian embryo flectin protein is predominantly expressed in the left epithelial cardiac compartment. After a short delay, the protein is expressed in the right cardiac compartment. This left–right delay in expression leads to the observed left-dominant, asymmetric pattern in the avian heart that correlated closely with looping (Tsuda et al., 1996, 1998; Linask et al., 2002, 2003a,b, 2005a). Subsequently, we demonstrated, as had been shown earlier for rat embryos (Baldwin and Solursh, 1989), that when the cardiac jelly extracellular matrix is removed, chick hearts continue to bend (Linask et al., 2003b). We, therefore, deduced that the continuing intracellular expression of flectin expressed within the myocardiocytes of the heart wall and in the developing outflow region as it forms from the second heart field, is closely associated with the bending and rotation of the heart tube.

Flectin was first localized using a monoclonal antibody Mab F22 that was cloned from a panel of antibodies

[1]Department of Pediatrics, USF/ACH-Children's Research Institute, St. Petersburg, Florida
[2]Fox Chase Cancer Center, Philadelphia, Pennsylvania
[3]Thomas Jefferson University, Philadelphia, Pennsylvania
[4]Wellcome Trust Centre for Human Genetics, University of Oxford, United Kingdom
[5]Department of Pathology, All Children's Hospital (ACH), St. Petersburg, Florida
Grant sponsor: American Heart Association; Grant sponsor: Suncoast Cardiovascular Research and Education Foundation.
†Dr. Seeholzer's present address is Proteomics Core, Children's Hospital of Philadelphia, Philadelphia, PA.
‡Dr. Farthing's present address is Cambridge University, Cambridge, UK.
***Correspondence to: Kersti K. Linask, USF/ACH Children's Research Institute, CRI 2007, 140-7th Avenue S., St. Petersburg, FL 33701. E-mail: klinask@health.usf.edu**

DOI 10.1002/dvdy.21645
Published online 11 August 2008 in Wiley InterScience (www.interscience.wiley.com).

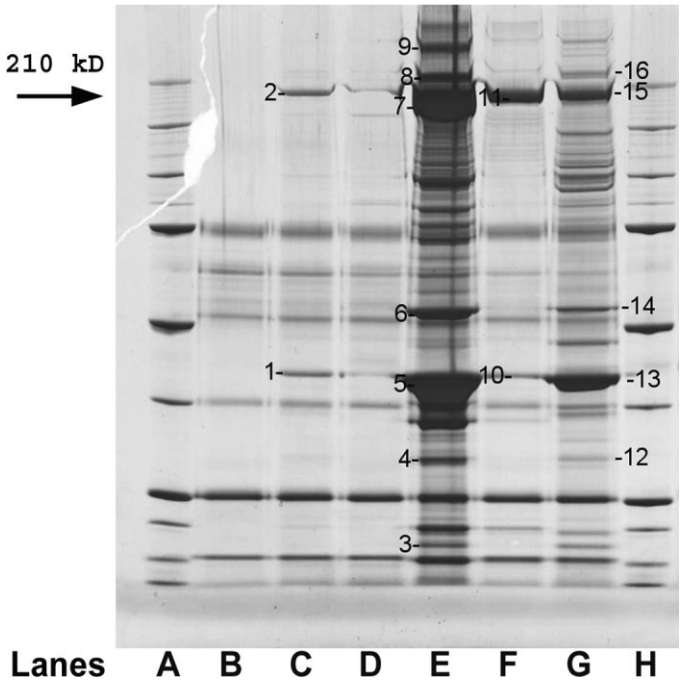

Fig. 1. Annotated Coomassie Blue stained gel resulting from immunoprecipitation (IP) with flectin antibody. Lanes are as follows: A, protein size markers; B, nonspecific protein binding; C, chicken embryo extract; D, colon HCT116 cytoplasmic extract; E, 10T1/2 nuclear extract; F, 10T1/2 cytoplasmic extract; G, HCT116 nuclear extract; H, protein size markers. The numbers indicate the different protein bands identified using MALDI-MS. Proteins identified and accession numbers are provided in Table 1.

generated from a mouse immunized with detergent insoluble cytoskeletal proteins isolated from embryonic day18 chick retinal pigment epithelium (RPE; Lash et al., 1992). The antibody was found to cross-react with a highly conserved protein around a molecular weight of 240 kDa and found in the interphotoreceptor matrix (IPM) of vertebrate eyes (Mieziewska et al., 1994). The IPM is found in the subretinal space, which is bordered by the apical surface of the RPE and the outer-limiting membrane of the neural retina. During development, apical cell processes of RPE cells and Muller glial cells, as well as the inner and outer segments of the photoreceptor cells extend into this space. The IMP facilitates retinal adhesions and the trafficking of metabolites between the RPE and neural retina. The IPM is composed of glycoproteins, proteoglycans, and glycosaminoglycans (Hollyfield, 1999). Likewise in the cardiac jelly, hyaluronan and hyaluronan binding proteoglycans are highly expressed in this extracellular compartment of the heart. Subsequently, we designated this protein "flectin" based upon the Latin word *flectere*, to bend or to loop (Tsuda et al., 1996), because in the early chick and mouse embryo it is often expressed, although not exclusively, in epithelial structures that are bending or changing shape, as during somitogenesis (Lash et al., 1992). Flectin is expressed also by the endocardial endothelial cells and by the cephalic migrating neural crest cells (Tsuda et al., 1996).

To isolate and identify flectin protein, it was necessary to obtain large enough quantities of protein for biochemical assays. Therefore, in addition to embryonic chick and mouse tissue, we determined other cells/tissues from other vertebrates that expressed protein reacting with F22 antibody. As described in this report, these included the mouse fibroblast 10T1/2 cell line and a human colorectal carcinoma cell line. Using MALDI-Mass spectrometry, we identified flectin antibody reacting with the nonmuscle myosin II class of proteins in all cell types. This class of proteins is integral to actomyosin interactions, to cilia and involved with mechanotransduction and is a seemingly logical protein complex to be involved in heart tube bending. The well recognized intracellular cross-talk between cell–cell adhesion and cell–matrix interactions to coordinate development of form and function (Linask et al., 2005b) suggested that proteins associated with the cytoskeleton facilitate heart looping.

RESULTS

MALDI-Mass Spectroscopy and Proteomic Identification of Flectin (FL) as a Nonmuscle Myosin-II Protein

Identification of chick flectin protein was carried out using immunoprecipitation (IP) with the monoclonal IgM flectin (F22) antibody of proteins with cell extracts of whole chick embryos, as well as of embryonic hearts separately, at HH stages 12–14 (Hamburger and Hamilton, 1951). Between these embryonic stages, flectin is expressed at high levels in the looping heart, as well as in the neural tube, notochord, neural crest cells, foregut, in the outer epithelium where lateral walls are bending to encompass the embryo, and in cells of the extraembryonic splanchnopleure enclosing the embryo (Tsuda et al., 1996, 1998). To facilitate protein identification in different vertebrate groups, we identified and localized flectin in mouse embryonic tissue and in human and mouse cell lines. We prepared cell extracts and similarly carried out IPs. Flectin expression in a human colorectal carcinoma HCT116 cell line and the mouse embryonic fibroblast 10T1/2 cell line displayed variable subcellular compartment localization.

After sodium dodecyl sulfate-polyacrylamide gel electrophoresis (SDS-PAGE), multiple specific proteins were detected to co-immunoprecipitate with flectin in the chick embryonic hearts and mouse and human cell lines (Fig. 1). The specific co-immunoprecipitating protein results are shown in Table 1. Based upon previously published evidence, we expected a band in the 200- to 250-kDa range for flectin (F22; Lash et al., 1992). The SDS-PAGE consistently showed a protein with a molecular weight of 210 appearing in all fractions relative to a control lane of nonspecific binding. Selected protein bands, specifically the 210-kDa protein band and those that co-immu-

TABLE 1. Proteins Co-Immunoprecipitating with Flectin Antibody

Sequence Name	ID Number	Annotated Numbers
Actin, cytoplasmic 2 (gamma actin)	P63261	1, 5, 13
Nonmuscle cellular myosin heavy chain, type A	P35579 (Homo)	15
Cellular myosin heavy chain	P14105 (Gallus)	2
Nonmuscle myosin type A	Q62812 (Rattus)	7, 11
Calmodulin (CaM)	P62157	3
Tropomyosin 3	P06753	4, 12
Vimentin	P20152	6, 14
Filamin A	Q8BTM8	8
Plectin 1	P30427	9
Cytokeratin 10	P13645	10

noprecipitated were sequenced by MALDI-TOF-mass spectrometry (MS). The 210-kDa bands were all identified initially as cellular nonmuscle myosin heavy chain-IIA. Identification of flectin antibody as an intracellular protein of the nonmuscle myosin II class suggested that it would interact and possibly be complexed with other cytoskeletal molecules. This was the case, as shown in Table 1. The MALDI-MS data identified the other specific coimmunoprecipitating bands as cytoskeletal-associated proteins: actin, calmodulin, tropomyosin, vimentin, filamin, plectin.

EGFP-NMHC-IIA and -IIB Transfection Analyses

To validate the specificity of the commercially prepared peptide antibodies and to determine the possibility that flectin was recognizing both NMHC-IIA and NMHC-IIB, we transfected 10T1/2 cells with full-length human NMHC-IIA-GFP or NMHC-IIB-green fluorescent protein (GFP) -expressing constructs. All cell lines that we analyzed, endogenously expressed one or both NMHC-II proteins. Thus, our focus was on whether the specific GFP-expressing protein was detectable by the specific antibody. After transfection, we fixed the cell cultures and immunostained with commercial antibodies or with flectin antibody. Shown at higher magnification (Fig. 2), it is observed that the commercial antibodies made against mouse protein are specific for the respective NMHC-II isoform (Fig. 2; first plate on left), is for NMHC-IIA antibody reactivity; middle plate for NMHC-IIB reactivity; and plate on right is for flectin F22 antibody reactivity). Flectin antibody, however, recognized both human isoforms, albeit more weakly (last plate), possibly reflecting that flectin antibody was made against chicken protein and is specifically different from the mouse and human protein in the carboxy end of the molecule. The epitope that the antibody is recognizing we currently do not know and will be an area of future investigation.

Protein Identification Verified by Western Blotting and Reverse Transcriptase-Polymerase Chain Reaction

Western blots were carried out with the commercially available polyclonal rabbit anti-nonmuscle myosin heavy chain (NMHC) -IA and -IIB antibodies using the different cell extract proteins and from different cellular compartments transferred onto nylon membranes.

Nonmuscle myosin-IIA.

Figure 3A shows an immunoblot of stage 12 chick embryonic heart cell lysates, of 10T1/2 mouse cells, with and without immunoprecipitation using flectin antibody, and of human HCT 116 cells. In all cases, the same 210-kDa NMHC-IIA protein is detected (lanes 1–7). Lane 8 is a positive control of the NMHC-IIA protein immunoprecipitated from the adult mouse eye. Whole mouse embryos on embryonic day (ED) 9.5 express NMHC-IIA (lane 9, no IP; and lane 10, with flectin IP).

Nonmuscle myosin-IIB and -IIC.

Previously, we demonstrated that NMHC-IIB is present during chick myocardial differentiation using precardiac mesoderm explant cultures to analyze myofibrillogenesis (Du et al., 2003). We, therefore, analyzed the possibility that NMHC-IIB may also be present in the directly loaded samples or in the flectin antibody immunoprecipitates, because the flectin antibody appeared to be recognizing a common epitope on the two isoforms (Fig. 2). NMHC-IIB was present in the 210-kDa band using cell extracts from mouse embryos or the human HCT 116 cells and mouse cell lines (Fig. 3B). NMHC-IIB positive control is seen in lane 1 in cell extract of adult mouse brain. We also analyzed the embryonic and cell lysates for NMHC-IIC (using an antibody recognizing the carboxy terminus of the protein). NMHC-IIC was not present in the embryos, as based on immunohistochemistry and by reverse transcriptase-polymerase chain reaction (RT-PCR; not shown).

Early mouse embryonic hearts express NMHC-IIA, contrary to what had previously been reported based on Western immunoblots (Tullio et al., 1997). In the cited study, because of possible problems with level of detectability using Western blots, we analyzed for NMHC-IIA mRNA using RT-PCR for expression at different stages throughout chick heart development (Fig. 4) and for protein expression immunohistochemically at ED9.5 in mouse embryo (Fig. 5). RT-PCR data indicated that at all developmental time periods analyzed between primitive streak stage 5 and embryonic day 18, NMHC-IIA mRNA was present in the chick heart fields (HH stage 5/8) or in the heart (HH stage 12 up through 18 days after fertilization). We did not carry out a temporal expression analyses on the mRNA in the mouse, because the knockout mouse displayed embryonic lethality on ED7.5 (Conti et al., 2004), already indicating that NMHC-IIA would have to be expressed early in the embryo.

Both NMHC-IIA and -IIB Are Expressed in the Embryonic Mouse Heart

Using Vectastain horseradish peroxidase localization (Fig. 5, brown signal) of NMHC-IIA, -IIB, and flectin in adjacent sections of an ED9.5 mouse embryo, in comparison to the negative

Developmental Dynamics

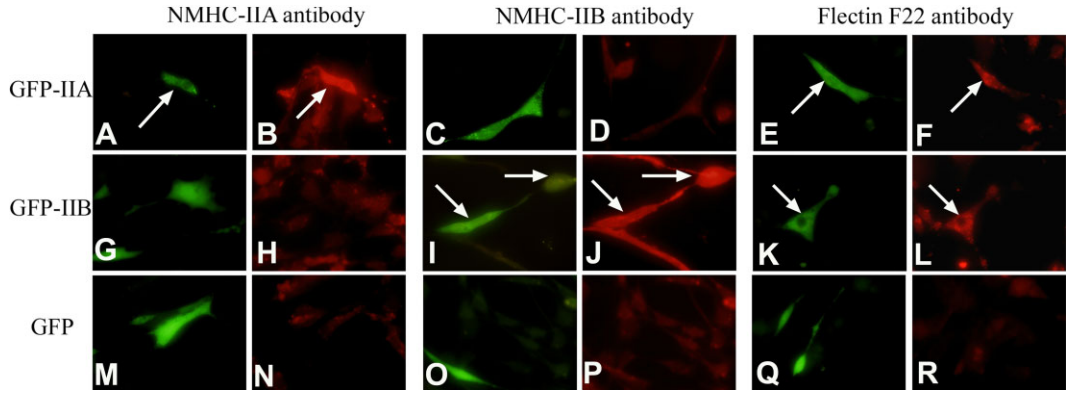

Fig. 2. Immunostaining of 10T1/2 cells transfected with green fluorescent protein (GFP)-tagged full-length human NMHC-IIA or -IIB. The GFP-tagged-NMHC-II (green signal) and respective NMHC-II immunolocalization by Texas Red conjugated-secondary antibody (red signal) is shown in adjacent panels. **A,B:** A more intense signal (see arrows) is detectable when the transfection of the full-length specific GFP-NMHC-IIA (top row) or GFP-IIB (middle row) matched the primary antibody (Ab) that was used for immunostaining (NMHC-IIA antibody; and I,J for NMHC-IIB, respectively). **C,D,G,H:** A background Texas red signal could be observed in IIA transfected cells stained with anti-IIB antibody (C,D) or vice-versa (G,H). **E,F,K,L:** The flectin F22 monoclonal antibody recognized an epitope common to both NMHC-IIA (E,F) and NMHC-IIB (K,L) protein. The Texas Red signal was at background levels in the cells transfected with the plasmid carrying the GFP sequence only (bottom row). It is noted that these cells express different levels of the endogenous protein (i.e., non–GFP-expressing).

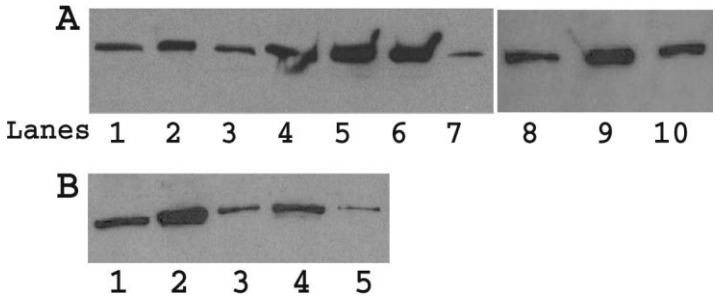

Fig. 3. Immunoblots of chick and mouse embryo extracts and of cell lines. Blots were probed using antibodies to human peptides of NMHC-IIA and NMHC-IIB. **A:** NMHC-IIA immunoblots: NMHC-IIA antibody detects the 210-kDa protein in *directly loaded* (*no IP*) lysates of chick Hamburger and Hamilton (HH) stage 12 heart (lane 1); and of HH stage 12 whole chick embryo (lane 2); mouse 10T1/2 cell cytoplasmic fraction (lane 3); mouse 10T1/2 cell enriched nuclear fraction (lane 4); human HCT116 cytoplasmic fraction (lane 5); human HCT116 enriched nuclear fraction (lane 6); and chick embryonic stage 16 heart fraction (lane 7). On another gel, adult mouse eye IP, a positive control lane for murine NMHC-IIA (lane 8); mouse embryo ED9.5, no IP (lane 9); and ED9.5 mouse embryo, flectin IP (lane 10). **B:** NMHC-IIB immunoblots. Lane 1, lysate from adult mouse brain (positive control); lane 2, mouse embryo, no IP; lane 3, mouse embryo, after IP with FL mAb; lane 4, human HCT 116 cytoplasmic fraction, no IP; and lane 5, after IP.

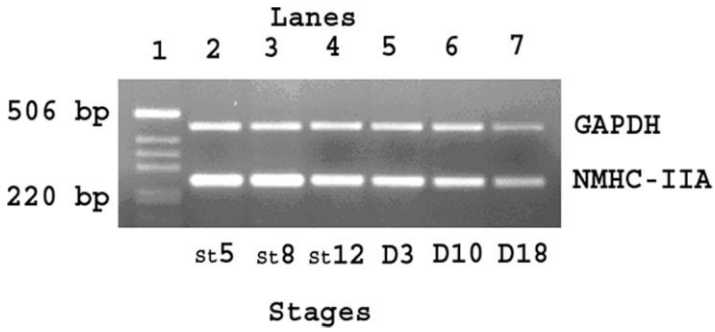

Fig. 4. Reverse transcriptase-polymerase chain reaction shows presence of NMHC-IIA mRNA in embryonic chick heart-forming regions and hearts at all stages analyzed (bottom row): Hamburger and Hamilton (HH) stages 5, 9, 12, and days 3, 10, and 18. Top row shows glyceraldehyde-3-phosphate dehydrogenase (GAPDH) as a loading control.

control (Fig. 5A–C), both NMHC-IIA (Fig. 5D–F) and -IIB (Fig. 5G–I) are expressed in the heart. Specifically, both localize in the myocardium and endocardium on ED9.5 (Fig. 5D,E and G,H). There is little NMHC-IIA expressed in the neural crest region (Fig. 5F) in contrast to the higher expression detectable of NMHC-IIB (Fig. 5I). Flectin expression (Fig. 5J–L) is more similar to NMHC-IIB in that it shows high expression in the myocardium (Fig. 5K) and neural crest (Fig. 5L). In addition flectin, however, recognizes apparent fibrils or cell extensions within the cardiac jelly (Fig. 5K) that NMHC-IIB antibody does not, although such cell processes or fibrils extending into the cardiac jelly appear to be present in the control embryonic heart (see green arrow). Cells in the same ventral region

Fig. 7. A,B: Three-dimensional reconstruction of the semitransparent myocardial wall (pink color) and endocardial lumen (blue) of a stage 14 looping chick heart (A) and one section (B) depicted through the inflow part of the heart in diastole (green arrow); ventricular part is in systole (orange arrow). Myocardial wall (white) was immunostained with MF20. Double-headed red arrow defines extent of region where endocardium is closely apposed to the myocardial wall on the ventral and dorsal sides during blood filling the heart. Seemingly, there is significant displacement of the cardiac jelly during the cardiac cycle. Ventral floor of the foregut (FG) is shown for embryonic midline position. Scale bar = 100 μm.

Developmental Dynamics

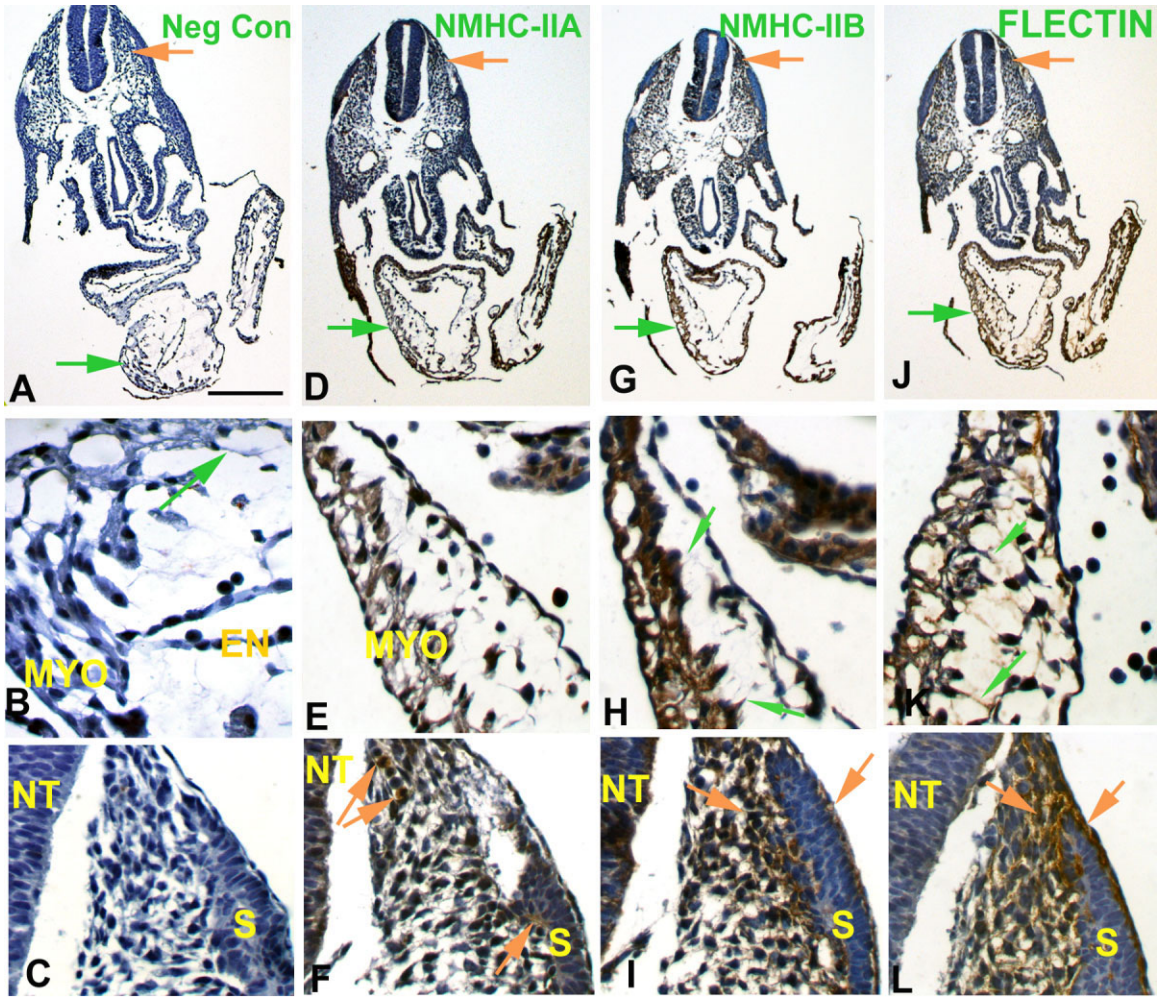

Fig. 5. NMHC-IIA, NMHC-IIB, and flectin localization in adjacent sections of mouse embryonic hearts on embryonic day (ED) 9.5. **A–C:** Sections for the negative control are from a different ED9.5 embryo. **D–F:** NMHC-IIA localizes primarily to the heart (D,E) and only a few cells are seen to be positive in the neural crest pathway (in A, orange arrow; in F, see two orange arrows). **G–L:** Ventral cells in panel F of the somite (S) region also express NMHC-IIA. NMHC-IIB (G–I) and flectin (J–L) show similar localization patterns in the heart (G,J; green arrows) and in the neural crest (orange arrows). At higher magnification of the heart (H,K), there is a high level of expression in the myocardium (MYO) and also in the inner curvature of the heart. Flectin antibody that was made against chick protein, shows a lower level of reactivity to mouse protein, but localizes similarly to the myocardium, as well as in the inner curvature of the heart. Unlike NMHC-IIB antibody, flectin antibody, however, localizes as seen in K to fibrils or cell processes extending between cells within the cardiac jelly region (green arrows). Similar light-blue staining fibrils or processes are also apparent in the negative control sections (green arrow in B). In a like manner, NMHC-IIB and flectin also localize at high levels within the neural crest migration pathway (I,L), in association with the ventral side of the somitic region where cells will begin to migrate out, and in the overlying epidermis (orange arrows). MYO, myocardium; EN, endocardium; NT, neural tube; S, somite. Scale bar = 400 μm in A for top row, 40 μm in B, for middle and bottom rows.

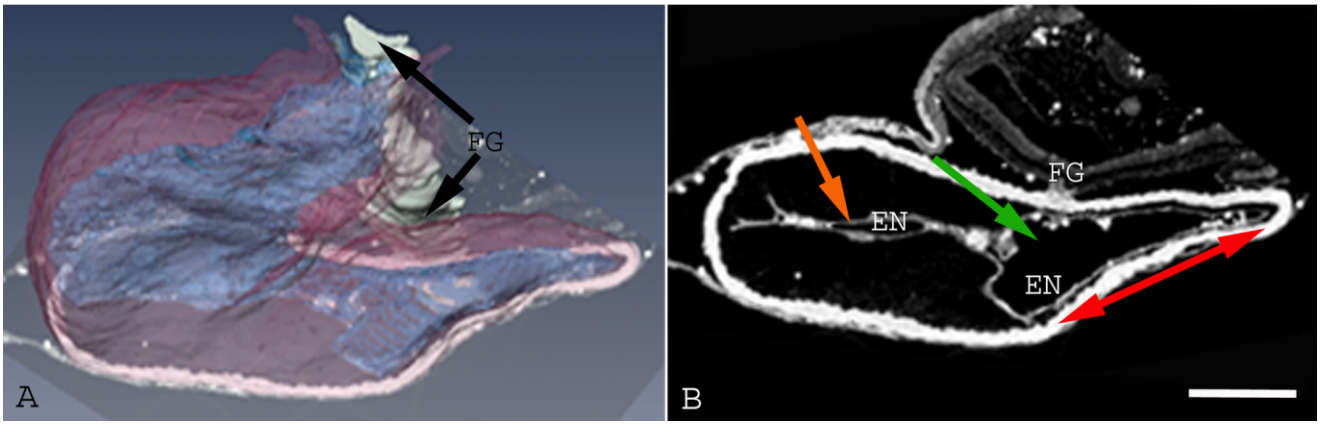

Fig. 7.

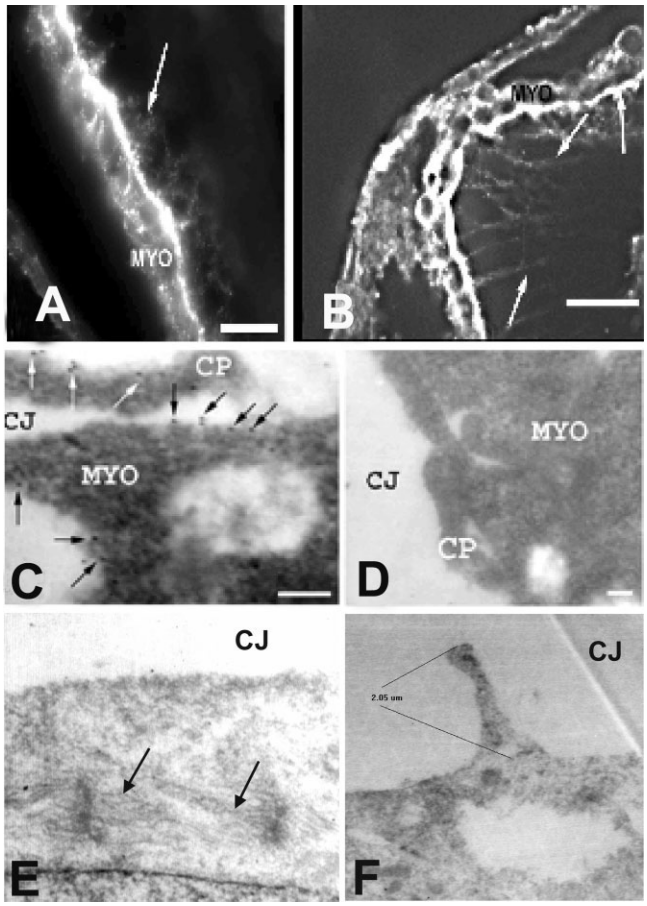

Fig. 6. Immunolocalization of flectin within the chick embryonic myocardium and cell processes or fibrils extending into the cardiac jelly. **A,B:** Flectin localizes to the myocardium (MYO) and basal layer of the wall and within the adjacent cardiac jelly (arrows). In regions of the heart tube bending, the cell extensions/ fibrils extend some distance into the cardiac jelly. **C:** Electron micrograph of immunogold labeling (10-nm particles) showing flectin in the cytoplasm of the cardiomyocyte (black arrows) and in a cell process (CP; white arrows) extending from the myocardiocyte (MYO) into cardiac jelly (CJ). **D:** Section of control heart wall exposed to immunogold antibody only with no primary antibody treatment. No immunogold particles were apparent in the control specimen. **E:** In this section through control heart, sarcomeres are forming (arrows) with Z-bands apparent and myofibrils in basal layer are circumferentially oriented with respect to the heart tube. **F:** A cell process of 2.5 μm extending into the cardiac jelly from the myocardial wall. Scale bar = 50 μm in A,B, 100 nm in C,D, 1 μm in E,F.

of the somite also localize NMHC-IIA, -IIB, and flectin.

Flectin Localization in Cardiomyocyte Cell Processes Extending From the Myocardial Wall Into the Cardiac Jelly ECM

In the nonmuscle myosin literature, NMHC-II proteins are described as being motor proteins, associated with actin in the cytoskeleton and are present in certain cell contexts in cell processes as filopodia and microcilia. This suggested that NMHC-II may be present in cell processes or filopodia extending from the basal surface of the myocardiocyte and may interact closely with ECM molecules in the microenvironment. We used both confocal and electron microscopy to analyze for the presence of cell processes on cardiomyocytes (Fig. 6). Two types of cell processes were apparent, very short ones ~1 to 3.0 μm in length and longer cell extensions, possibly similar to cytoplasmic stress fibers previously reported in the embryonic heart at later stages (Sumida et al., 1989). Flectin (NMHC-IIB) is highly expressed at the basal side of the myocardial wall and extending into the adjacent matrix of the basal lamina (Figs. 5B,H,K, 6A,B).

Short cell processes.

We used flectin antibody and immunogold labeling of chick embryonic hearts to determine using electron microscopy whether short cell processes exist on the basal aspect of cardiomyocytes and whether flectin (NMHC-II) localizes intracellularly within these processes. The antibody recognizing the mouse NMHC-IIB peptide does not recognize chick protein, hence, we used flectin antibody that is made against the chick protein. Immunogold labeling of flectin antibody was detectable in the cytoplasm of the basal cardiomyocytes and in a short cell process (CP; Fig. 6C; arrows pointing to 10-nm immunogold labeling). In a control embryo incubated with secondary gold-conjugated antibody only, no labeling was seen in a cell process (Fig. 6D). In some of the basal cardiomyocytes, the circumferential organization of sarcomeric myofibrils is apparent, as previously reported (Fig. 6E). In many cardiomyocytes, cell processes of 1–3 μm in length extending from the surface of cardiomyocytes into the cardiac jelly (CJ) were apparent, but were sparsely localized in these thin sections (Fig. 6C,D,F). These short cell processes are not microcilia, as they do not localize tubulin (Linask and VanAuker, 2007).

Cardiac Jelly Displays Significant Compressibility and Displacement During the Cardiac Cycle

That the cardiac jelly compartment alters shape and seemingly shows compression or is displaced during contraction and relaxation of the heart wall during the cardiac cycle is seen in sections that were used to three-dimensionally reconstruct a MF 20 immunostained, chick HH stage 14 looping heart that was embedded in plastic and sectioned at 3 μm (Fig. 7A,B). As observed, the endocardium (blue) is not a smooth, central cylinder surrounded by a wide expanse of cardiac jelly, as often depicted in papers and textbooks, but shows differential shapes and outpocketings during heart contractions. The endocardium is closely apposed to the myocardial wall in specific regions (B; red arrows) of the looping heart within the cardiac

cycle. The potential for blood flow forces on the endocardial wall to be transmitted to the myocardial wall appears real, as the myocardium during relaxation of the heart tube (diastole) is closely apposed to the underlying endocardium as blood enters the heart. Little cardiac jelly extracellular matrix (ECM) now exists between the myocardial/endocardial layers in the inflow part of the heart during cardiac filling during diastole (region depicted by red line with double arrows). Figure 7B shows the cross-section for the specific region described in the three-dimensional (3-D) reconstructed heart.

Flectin and NMHC-IIB Are Modulated in the *Nodal*$^{\Delta 600}$ Embryonic Heart

Flectin was previously shown to be modulated by misexpression of Pitx2c and CFC in the chick embryonic heart (Linask et al., 2002, 2003a). To validate presently in the mouse model our previous data on misexpression of Pitx2c/CFC and flectin modulation(Linask et al., 2002, 2003b), we determined whether NMHC-IIB protein expression in the transgenic *Nodal*$^{\Delta 600}$ mouse heart similarly is modulated. We chose to analyze *Nodal*$^{\Delta 600}$ homozygous embryos because with the deletion of the ASE enhancer region the dynamic patterns of Nodal expression are modulated during mouse development and only a weak level of Nodal expression is apparent in the left lateral plate mesoderm (Norris et al., 2002). These *Nodal*$^{\Delta 600}$ homozygous embryos display an asymmetric, but slightly delayed, as well as much restricted, Pitx2 expression in the heart region. By ED9.0, looping is visibly abnormal. To confirm that NMHC-IIB is associated with asymmetry and the laterality pathway in the mammalian mouse heart, we immunolocalized flectin or NMHC-IIB in the Nodal$^{\Delta 600/\Delta 600}$ embryos (Fig. 8); nonspecific background binding of secondary antibody was apparent in the gut tube only and is shown in panel 8C,F, when no primary antibody was used. We expected a reduced level of expression of NMHC-IIB due to only a weak level of Nodal expression in the homozygous animals. This we observed on both protein and mRNA levels. In comparison to flectin localization in the wild-type (Fig. 8A in whole-mount; section through heart shown at low [Fig. 8D] and higher magnification in Fig. 8G), the Nodal$^{\Delta 600/\Delta 600}$ hearts showed a reduced level of expression of flectin (Fig. 8B, E, and H, respectively). The punctate localization in the transgenic embryo is real in that it is seen only in association with cells and not on background. Similar reduced expression was observed in relation to NMHC-IIB specific antibody localization in the Nodal$^{\Delta 600/\Delta 600}$ embryo in comparison to the wild-type (compare Figs. 8I, K, and M of +/+ heart with Fig. 8J, L, and N showing much reduced NMHC-IIB expression in the Nodal$^{\Delta 600/\Delta 600}$ embryo). In the wild-type embryo it is noted that the myocardial wall is thicker (Fig. 8M) than seen in the homozygous mutant (Fig. 8N). Most of the intense signal near the heart wall in Figure 8M (+/+) or notably in 8N (Nodal$^{\Delta 600/\Delta 600}$) is due to the high level of expression of NMHC-IIB in the splanchnopleural (sp) membrane closely apposed to the heart during looping. The reduced myocardial expression was also noted using RT-PCR analyses of NMHC-IIB expression in the Nodal$^{\Delta 600/\Delta 600}$ embryo in comparison to wild-type (anterior halves of embryos used only). Inset of RT-PCR gel data: Densitometric ratios of NMHC-IIB expression to housekeeping gene glyceraldehyde-3-phosphate dehydrogenase (GAPDH) gene expression intensities in wild-type was 0.93 (42.72/46) vs. in the Nodal$^{\Delta 600/\Delta 600}$ embryo with a ratio of 0.38 (60.55/159.45), as determined using the Kodak Gel Logic 100 System. Therefore, a ~ 2.4-fold reduction in NMHC-IIB message was noted in the transgenic Nodal$^{\Delta 600/\Delta 600}$ mouse model.

Heart Function of the NMHC-IIB null (NMHC-IIB$^{-/-}$) and Heterozygous (NMHC-IIB$^{+/-}$) Embryos Is Abnormal in Comparison to Wild-type (NMHC-IIB$^{+/+}$) Littermates

Previous characterization of phenotypic abnormalities of the NMHC-IIB null embryos reported that the observed anomalies reflected abnormal looping (Tullio et al., 1997). These observations suggested to us that heart function in embryos lacking NMHC-IIB may have been comprised. This we found to be the case. Using noninvasive echocardiography to monitor embryonic mouse heart function, both NMHC-IIB null embryos and heterozygotes display abnormal echo patterns (Fig. 9). In Figure 9A, the wild-type littermates on ED15.5 show normal inflow and outflow Doppler ultrasound patterns. In comparison the NMHC-IIB$^{-/-}$ (Fig. 9B) embryo displays abnormal inflow E/A ratios, as well as atrioventricular valve regurgitation. Additionally, the NMHC+/− (Fig. 9C) littermates show outflow related semilunar valve regurgitation, suggesting that even reduced levels of NMHC-IIB can affect cardiogenesis.

DISCUSSION

Cytoskeletal restructuring is required for cell shape changes, for the movement of cells, and for the shaping of tissues throughout morphogenesis. Cells depend on cytoskeletal molecules and molecular motors to establish their asymmetrical shapes and to drive cell motility (Pollard, 2003). Heart organogenesis requires cell migrations (Linask and Lash, 1986, 1988), cell shape changes (Linask, 1992a,b; Linask et al., 1997), and the bending of epithelial sheets to form a tubular structure (Linask et al., 2005a). The straight heart tube bends and rotates forming the definitive four-chambered organ (Linask and Lash, 1998; Linask, 2003). The anterior–posterior and dorsal–ventral patterning of cell–cell and cell–matrix adhesion molecules and their activity in signal transduction pathways are key in coordinating the development of cardiac form with function (Linask, 2003; Linask and VanAuker, 2007).

Nonmuscle Myosin II Proteins and Heart Looping

On the basis of the present study, the cross-talk between the cell adhesion molecules, cell–cell and cell–matrix, during looping is facilitated by the actomyosin cytoskeletal complex and signaling, that involves nonmuscle myosin IIB, and possibly NMHC-IIA, in the myocardium. Knockout mice of NMHC-IIB and NMHC-IIA had been generated (Tullio et al., 1997; Conti et al., 2004)

previous to our identification of flectin antibody recognizing NMHC-IIA and -IIB isoforms in the heart. NMHC-IIA transgenic embryos displayed embryonic lethality at ED7.5 (i.e., early heart compartmentalization stage). The NMHC-IIB null transgenic mice were described as displaying heart looping defects and usually surviving to midgestation (Tullio et al., 1997). However, in those studies an analysis of NMHC-IIA and -IIB expression during earlier, heart looping, stages was not done, nor was the effect on heart function defined. Indeed possibly because of level of detectability of their Western blot data, it was indicated previously that NMHC-IIA was not present in the heart during development, unless NMHC-IIB was knocked out and then was up-regulated (Tullio et al., 1997). Our data indicate that both NMHC-IIA and NMHC-IIB isoforms are present already during the earliest stages of normal heart development and during looping.

Flectin antibody seemingly is a pan-NMHC-II antibody, as it interacts with both NMHC-IIA and NMHC-IIB. It also appears as seen in Figure 5 to be localizing to possibly a secreted isoform of NMHC-II in the cardiac jelly or alternatively, to cellular footprints or cell processes, as matrix molecules are being secreted to form the cardiac jelly by the myocardial cells (Manasek, 1976a). The commercial NMHC-IIA and -IIB antibodies are made against 12 amino acid peptides corresponding to the C-terminus of human nonmuscle myosin heavy chain isoform A and B that are also well conserved in the mouse, but differ in the chick isoforms. This finding also suggests the peptide antibodies may not bind to modified isoforms, as phosphorylated forms, or to secreted forms where cleavage of the secreted protein may have taken place. It is known that the phosphorylation status of myosin II is important in intracellular tension and is associated with stress fibers, whereby signaling can occur by means of the ROCK-RhoA-kinase pathway regulating the phosphorylation level of myosin II (Vemuri et al., 1999; Davis et al., 2001; Epstein and Davis, 2003; Kawabata et al., 2004). Interestingly, inhibition of Rho kinases by Y27632 blocks normal heart development and normal left–right asymmetry (Wei et al., 2001, 2002). We suggest this may occur by its leading downstream to an inhibition of nonmuscle myosin II phosphorylation. Flectin antibody on the other hand was made against cellular proteins and apparently recognizes a conserved region on both NMHC-IIA and -IIB, and it may bind to both phosphorylated and unphosphorylated isoforms. This allows detection of myosin II proteins in cells and cell processes when under tension or possibly even secreted under conditions where there is mechanical tension. The latter aspects are now being investigated in the looping heart. NMHC-IIB is reported to be in cell processes within lamellipodia/filopodia, and it is associated also with fibroblast collagen fiber transport and deposition during remodeling of the ECM (Meshel et al., 2005). Either tension fiber formation or matrix deposition could explain the seemingly extracellular and/or subepithelial localization initially reported for flectin-F22 protein (Lash et al., 1992). Myocyte cytoplasmic stress fibers have been previously reported in the matrix compartment of later stage embryonic hearts in the AP septum region and were described as morphological adaptations to mechanical tensions in the heart (Sumida et al., 1989). Both possibilities appear to exist for the embryonic looping heart stages.

Fibronectin (FN) and collagens localize to the myocardial basal lamina where we detect cardiomyocyte cell processes. Upon RGD-perturbation of integrin-mediated cell matrix interactions, heart development becomes abnormal (Lash et al., 1987; Yost, 1992). As a result of RGD-perturbation, flectin was reduced in its expression in the cardiac jelly region of the heart (Linask and VanAuker, 2007). This finding may be due to a weakening of integrin binding on the cell processes with the basal lamina FN, and leads to a retraction of the cell processes or filopodia. This possibility warrants further investigation. We hypothesize that NMHC-IIB in association with integrin-mediated signal transduction is involved in mechanotransduction of increasingly higher blood flow volumes that are feeding into the heart during looping. As an example, increasing blood pressure may be transmitted to the inflow part of the myocardial wall as seen in Figure 7 by the compression or displacement of the cardiac jelly. During the cardiac cycle, the forces of ECM compression/displacement seemingly can be detected and transmitted to the closely apposed myocardium by cell processes, even short ones that are extending into the cardiac jelly matrix during the cardiac cycle. Although degradation of the cardiac jelly by hyaluronidase allows looping to continue in the rat and chick models (Baldwin and Solursh, 1989; Linask et al., 2003b), this enzyme exposure would be expected to break down proteoglycans, but would not be expected to degrade integrin-glycoprotein interactions within the myocardial basal lamina that becomes closely apposed to the endocardium in these experimentally treated embryos. The association of NMHC-II proteins with mechanotransduction is seen in other systems, as for example, in relation to cilia in the inner ear for transmission of sound waves and in relation to afferent and efferent arterioles in the kidney in detection of blood flow pressure (Shiraishi et al., 2003; Marigo et al., 2004). Recently, with regard to mesenchymal stem cells the nonmuscle myosins are shown to

Fig. 8. A–N: Flectin localization (A,B; D,E; and G,H) and NMHC-IIB (I–N) in embryonic day (ED) 9.5 hearts of Nodal$^{+/+}$ and Nodal$^{\Delta 600/\Delta 600}$ embryos. Arrows point to the myocardium. A: Nodal$^{+/+}$ heart; sections in D (low magnification), and G (high magnification). Wild-type heart displays a higher signal in comparison to the transgenic Nodal$^{\Delta 600/\Delta 600}$ heart (B,E,H). C (bright-field) and F depict a negative control embryo using secondary antibody only. Nonspecific signal is apparent in gut tube. I and sections (K,M) of a Nodal$^{+/+}$ mouse heart display a normal level of NMHC-IIB with left-dominant NMHC-IIB protein expression; (M) same heart shown at higher magnification. J: Section of Nodal$^{\Delta 600/\Delta 600}$ depicts a heart displaying abnormal looping with a reduced level of NMHC-IIB expression. Sections (L,N) of another Nodal$^{\Delta 600/\Delta 600}$ heart showing similar reduced level of NMHC-IIB. Region in L (arrow) is seen at higher magnification in N. NMHC-IIB is detected chiefly in association with the outer myocardial (Myo) cell membrane. The splanchnic membrane (sp) apposed to the heart wall displays a high level of NMHC-IIB. Inset on right is of reverse transcriptase-polymerase chain reaction results: glyceraldehyde-3-phosphate dehydrogenase (GAPDH) gene expression in embryonic hearts in wild-type (+/+, lane 2) vs. Nodal$^{\Delta 600/\Delta 600}$ embryos (−/−, lane 3; i.e., loading controls); lanes (4) and (5) depict NMHC-IIB expression levels in wild-type (+/+) and Nodal$^{\Delta 600/\Delta 600}$ (−/−) hearts, respectively. Scale bars = 495 μm in AB,F,I,J, 497 μm in D,E,K, 140 μm in L, 75 μm in G,H,M,N.

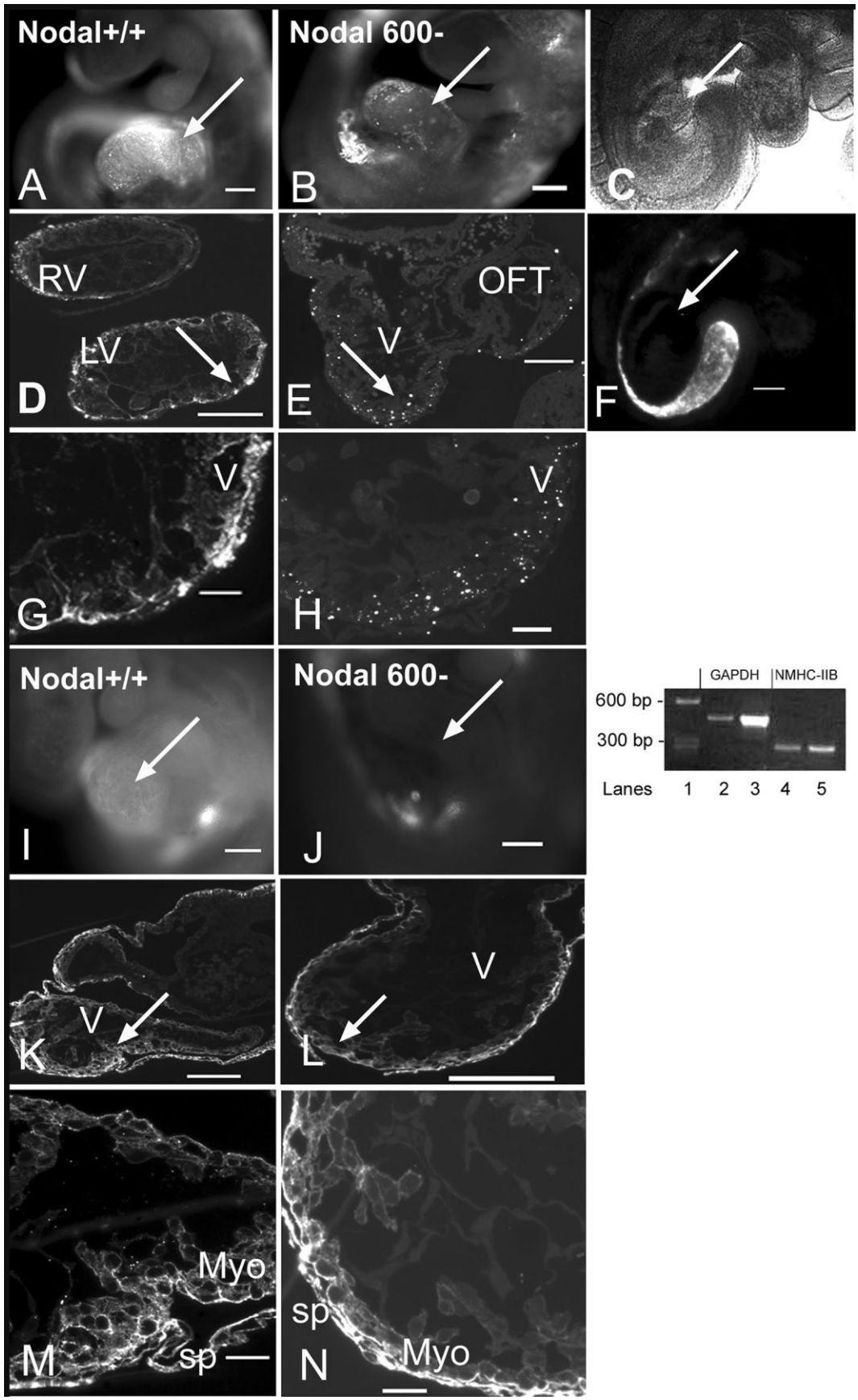
Nodal+/+
Nodal 600-
A
B
C
RV
LV
D
OFT
V
E
F
V
G
V
H
Nodal+/+
Nodal 600-
I
J
GAPDH
NMHC-IIB
600 bp -
300 bp -
Lanes 1 2 3 4 5
V
K
V
L
Myo
sp
M
sp
Myo
N

Fig. 8.

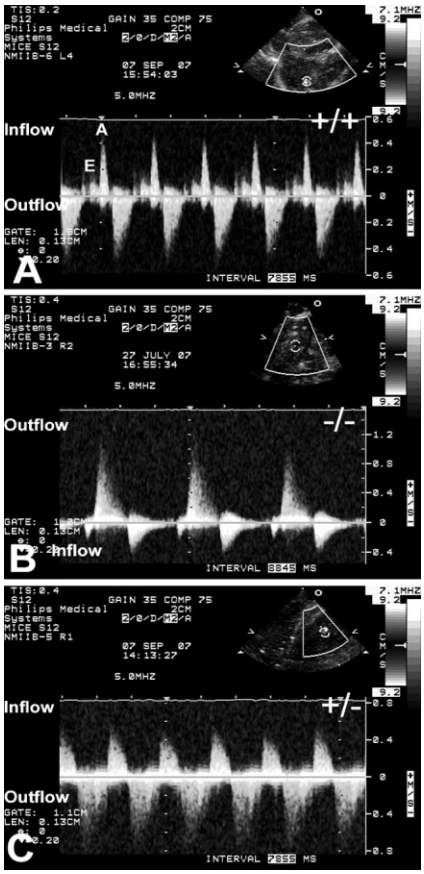

Fig. 9. NMHC-IIB heterozygous (+/−) and null (−/−) embryos display abnormal heart function as defined by Doppler ultrasound patterns acquired on embryonic day [ED] 15.5). **A:** Normal pattern of wild-type littermates (+/+) with E/A waves present. **B:** NMHC-IIB (−/−) embryos display abnormal inflow E/A waves and atrioventricular valve regurgitation. **C:** NMHC-IIB heterozygous (+/−) embryo showing semilunar valve regurgitation.

be involved in sensing matrix-elasticity to drive cell lineage specification (Engler et al., 2006). This feedback of local matrix changes on the cell state has important implications for development, differentiation, disease, and tissue regeneration (Discher et al., 2005; Linask and VanAuker, 2007).

Reduced Asymmetric Nodal Activity Leads to Abnormal Looping and Reduced Levels of Flectin/NMHC-IIB in the Heart

A downstream read-out of misexpression of upstream laterality regulatory genes has been the dextral direction and bending of heart looping. We determined that direction of heart looping is specified at approximately the seven-somite stage in the chick (Linask et al., 2005a) and suggested that the asymmetry of cell proliferation and flectin in the anterior heart field may relate to asymmetric patterning of Pitx2c (Ai et al., 2006). The laterality gene *Nodal* in all vertebrates analyzed shows a left expression in the embryo and heart fields and is upstream of Pitx2c. Reducing the level of Nodal in the left lateral plate mesoderm in the Nodal$^{\Delta 600/\Delta 600}$ embryo led to a restricted field of expression, as well as delayed expression of Pitx2c and abnormal cardiac looping at ED9.5 (Norris et al., 2002b). As we report here, the reduced Nodal expression in these transgenic mouse embryos resulted in a reduced expression of flectin and similarly of NMHC-IIB in the myocardium at ED9.5, detectable on both the protein and mRNA level. This study confirms in the mouse model our previous observations in the avian model on modulation of flectin by laterality genes during cardiac looping (Linask et al., 2002, 2003b).

Actomyosin Cytoskeleton and Heart Looping

The bending forces within the tubular heart appear to have a common underpinning related to tension and contractility of the cytoskeleton. Actin is a major component of looping (Manasek et al., 1972; Manasek, 1976b; Itasaki et al., 1991; Latacha et al., 2005). Development of actin filaments considerably differ in inner and outer myocardial cell layers (Shiraishi et al., 1992). In the inner layer at the tubular heart stage when the tube begins to bend, myofibrils are aligned with their long axis circumferentially arranged in relation to the tubular structure. Myocytes in the outer layer are round. It was suggested that the circumferentially arranged actin filaments at the basal aspect of the inner layer of the myocardium promote cardiac looping (Shiraishi et al., 1992; Price et al., 1996). Extracellular matrix protein fibronectin (FN) becomes aligned parallel with the actin bundles early in looping (Shiraishi et al., 1995). It is also this inner layer of cardiomyocytes that detectably sends cell processes, as well as secretes proteins, into the subjacent cardiac jelly layer. Additionally, a member of a the Ca++-dependent family of adhesion molecules, N-cadherin, is responsible for the connection of actin and myofibrils between neighboring myocytes at cell–cell junctions (Linask, 1992a; Kostetskii et al., 2005) and for the cell alignment and arrangement of the two layers of the developing heart tube (Shiraishi et al., 1993). Thus, during looping, as in the earlier period of cardiac compartment formation, cross-talk between two adhesion mediated-signaling pathways, integrin and N-cadherin, is evident (Linask and Lash, 1990; Linask, 1992b; Linask et al., 2005b) and as shown here, appears to be facilitated by the actin-nonmuscle myosin-II complex.

The identification of flectin as being more like nonmuscle myosin IIB localization during heart looping suggests the actomyosin cytoskeleton is involved in heart tube bending at a time that the myocardium is contracting and blood flow is present. We observed in the NMHC-IIB null embryo that heart function was compromised when compared with wild-type littermates, and may aid in the formation of the previously described cardiac anomalies (Tullio et al., 1997). NMHC-IIA apparently partially can compensate for NMHC-IIB, as a four-chambered heart does form, albeit abnormally. The abnormal cardiac function present in the heterozygous and homozygous embryos strengthens the hypothesis that there is a coordination of cardiac form with function during morphogenesis of the four-chambered heart (Linask, 2003).

Nonmuscle myosin-II proteins are important in morphogenesis throughout phylogeny. Evidence has been presented that nonmuscle myosins function in Drosophila in organizing the cytoskeleton during morphogenesis and in controlling left–right asymmetry (Blake et al., 1998, 1999; Speder et al., 2006). In summary, our study suggests that NMHC-IIB within the cytoskeleton has a role in laterality and mammalian mouse heart morphogenesis during looping.

EXPERIMENTAL PROCEDURES

Cells and Tissues

Chick embryos.

White Leghorn chick embryos (*Gallus gallus*) were incubated to HH stages 12–16 (Hamburger and Hamilton, 1951). For each experiment, whole embryos (~178–210 embryos) or microdissected embryonic hearts (268 hearts) were prepared for MALDI-MS analyses. C57Bl/6J mouse embryos at ED8.5 and ED9.5 also were analyzed.

Human and mouse cell lines.

Because of limitations of protein amounts obtainable from embryonic tissue, we also analyzed mouse and human cell lines that expressed flectin in either the cytoplasm, nuclei, or in both subcellular compartments. These sources included a mouse embryo fibroblast cell line (ATCC number CCL-226) and a human colorectal carcinoma cell line HCT116 (ATCC number: CCL-247).

Cell Extracts and Immunoprecipitation

Extracts of chick (260 HH stage 12) and mouse (40 ED9.5) whole embryos, embryonic hearts or cells were prepared and immunoprecipitation (IP) was carried out using flectin F22 monoclonal antibody: The embryos were placed into ice cold lysis buffer (50 mM Tris, PH 8.0, 5 mM EDTA, 150 mM NaCl, 0.5% IGEPAL CA-630) containing Protease Inhibitor Cocktail (Sigma-Aldrich, St. Louis, MO) and passed through a 21-gauge needle to break up the tissues and cells. Samples were kept on ice, vortexed, and centrifuged at 4°C for 10 min. The supernatant was collected. For cultured cells, cytoplasmic and nuclear fractions were prepared with NE-PER Nuclear and Cytoplasmic extraction Reagents (Pierce Biotechnology, Rockford, IL). Protein concentration was determined using Bio-Rad's protein assay (Bio-Rad Laboratories, Hercules, CA). Two mg of total protein was adjusted to 600 μl volume with lysis buffer, and incubated with 25 μl of rat anti-mouse IgM coupled-Sepharose 4B (Zymed, San Francisco, CA) for 30 min at 4°C, to remove nonspecifically binding proteins before forming the antibody-antigen complex. This mixture was centrifuged, supernatant removed, and 100 μl of mouse anti-chick flectin IgM antibody added. After mixing by rotation, 35 μl of rat anti-mouse IgM antibody coupled to Sepharose 4 was added and rotated for 4 hr to overnight for the IP. The immunoprecipitate/Sepharose complex was rinsed 3 times with lysis buffer and solubilized with sample buffer. After SDS-PAGE, the gel was stained with Coomassie Blue. An IP without addition of cell protein lysate served as a negative control. As an additional control another IgM monoclonal antibody for QH-1 was used for IPs and showed different bands immunoprecipitated.

MALDI Mass Spectroscopy

Selected protein bands in the gel were identified by MALDI-TOF-mass spectrometry (MS). Mass Spectrometry was performed as following: Protein bands were excised from colloidal Coomassie blue stained gels (Kang et al., 2002) and digested with trypsin after destaining, reduction, and alkylation (Shevchenko et al., 1996; Spodik et al., 2002). Recovered peptides were prepared for MALDI-TOF MS by mixing 1 μL of the peptide mixture with 2 μl of 30 μg/ml a-cyano-4-hydroxycinnamic acid (CHCA), 0.4% trifluoroacetic acid in 2:1 ethanol:acetone mixture and allowing the droplet to dry on the MALDI sample plate (Schuerenberg et al., 2000). In some cases, CHCA affinity sample preparation was used to improve sensitivity (Gobom et al., 2001). Peptide mass maps were obtained using a Bruker Daltonics (Bremen, Germany) Reflex IV MALDI-TOF mass spectrometer operated in positive ion reflectron mode. Proteins were identified from the peptide mass maps using Mascot (Matrix Science, London, UK; Perkins et al., 1999) to search the protein sequence databases.

Western Blots

We validated identification of flectin by Western blots using commercially available NMHC-IIA and NMHC-IIB specific antibodies (Covance, Berkeley, CA). Flectin antibody does not react in Western blots. SDS-PAGE was carried out with the immunoprecipitated proteins, as well as with proteins of the tissue and cell lysates used for direct blot (that is, no IP). For Western blots the proteins in the gel were transferred to a PVDF membrane (Bio-Rad, Hercules, CA) using a Mini Trans-Blot system (Bio-Rad). The membranes were dried, incubated in a dry milk-Tween/phosphate buffered saline (PBST) blocking solution, and were incubated with primary antibody in PBST. The membranes were washed in PBST followed by incubation with a donkey anti-rabbit IgG-horse radish peroxidase secondary antibody (GE Healthcare, Pittsburgh, PA). The filters were washed again in PBST and developed using enhanced chemiluminescence (ECL-plus) reagent (GE Healthcare). The primary antibodies used were (1) polyclonal nonmuscle myosin heavy chain IIA and nonmuscle myosin heavy chain IIB peptide antigen antibodies (Covance, Berkeley, CA) that recognize the carboxy regions of both human and mouse proteins. The antibodies were tested for their specificity as described in results. Because of sequence similarity the rabbit antibody binds well to mouse and human NMHC-II proteins, but weakly to chicken proteins in Western blots. Polyclonal rabbit anti-nonmuscle myosin heavy chain IIC antibodies made against the carboxy- and amino terminal ends of the protein were provided for our studies by Dr. R. Adelstein at NHLBI. These antibodies recognize both human and mouse nonmuscle myosin heavy chain IIC.

Immunohistochemistry and 3-D Reconstruction

Cells or embryos were fixed in 3.5% paraformaldehyde and immunohistochemistry was carried out a previously described (Imanaka-Yoshida et al., 1998; Linask and Tsuda, 2000). The horseradish peroxidase localization in Figure 5 was carried out using Vectastain ABC Kit from Vector Labs, Inc. (Burlingame, CA) according to their described protocol. Sections were analyzed with a Nikon Optiphot II microscope equipped for epifluorescence. Commercially prepared, polyclonal rabbit antibodies for short peptides of

NMHC-IIA, -IIB in the carboxy ends of the molecules were obtained from Covance. Flectin antibody was made against proteins in cellular extracts of the embryonic chick eye. The 3-D reconstruction was done using Amira software (Version 4.1; Mercury Solutions, Inc.) and 120 three micron Araldite plastic serial sections of a stage 14 looping chick heart immunostained for sarcomeric myosin heavy chain using MF20 antibody (Developmental Studies Hybridoma Bank).

Cell Culture and Transfection

10T1/2 cells were cultured in high glucose Dulbecco's Modified Eagle's medium (InVitrogen Gibco, Carlsbad, CA) supplemented with 10% fetal bovine serum (Gibco) and 1% antibiotic–antimycotic mixture (Gibco). Transient transfections with plasmid expressing the full-length human NMHC-IIA (Plasmid 11347; Addgene, Inc., Cambridge, MA) or NMHC-IIB (Plasmid 11348; Addgene, Inc.) coupled to enhanced green fluorescent protein (eGFP) or the eGFP alone were performed using Lipofectamine (InVitrogen). Two days after transfection, the cells were treated for immunostaining as follows. Cells were fixed at room temperature in PBS containing 2% formaldehyde and 0.2% glutaraldehyde, and blocked in a 1% bovine serum albumin/PBS solution. The samples were incubated with affinity-purified rabbit polyclonal antibodies to NMHC-IIA, IIB peptides (Covance), or the flectin F22 antibody overnight at 4°C. They were then incubated with a Texas Red-conjugated Goat anti-Rabbit IgG (Jackson Immunoresearch, West Grove, PA). Nuclei were counterstained with 4′, 6′-diamino-2 phenylindole (DAPI, Vector Laboratories, Burlingame, CA). The images were acquired using an Olympus IX71 fluorescent microscope.

Immunogold Labeling of Cell Processes and Electron Microscopy

Isolated stage 12 chick embryos were used for immunogold labeling. Embryos were fixed in Karnovsky's fixative and incubated with primary and secondary antibodies at 4°C overnight; rinsed well with PBS followed by PBS/bovine serum albumin rinses. Immunogold secondary antibody (Ted Pella, Inc) was conjugated with 10-nm gold particles. After rinses in PBS, postfixation was carried out with 2% glutaraldehyde in PBS. Embryos were rinsed with PBS, dehydrated in ethanol, embedded in Epon-812, thinly sectioned at 85 Angstroms, and sections placed on copper 300-mesh grids. Some sections were double-stained using uranyl acetate and lead citrate. Sections were viewed with a JEOL 1210 electron microscope.

RNA Extraction and RT-PCR Analysis

Total RNA was prepared from chicken embryonic heart-forming regions or hearts at different developmental stages (stages 5, 8, 12, day 3, day 10, day 18) using RNAeasy mini RNA kit (Qiagen, Valencia, CA) followed by treatment with RNase-free DNase (Promega Corp., Madison, WI). For cDNA synthesis, random hexamer primers were used for the reverse transcriptase (RT) reactions. The cDNA synthesis was carried out using AMV reverse transcriptase (Life Science, Inc.). To analyze relative expression of the different mRNAs, the amount of cDNA was normalized based on the signal from ubiquitously expressed GAPDH mRNA (450-bp product). The PCR was carried out using standard protocols with PCR Supermix (Invitrogen, Carlsbad, CA) and the following cycling parameters: denaturation at 95° C for 30 sec, annealing at 53–55°C for 1 min depending on the primer, and elongation at 72°C for 1 min; number of cycles varied between 30 and 35, depending on the abundance of the particular mRNA. The number of cycles and the amount of cDNA was chosen in such a way as to select PCR conditions on the linear portion of the reaction curve avoiding "saturation effects" of PCR. The identity of the PCR products was confirmed by sequencing. Primer sequences (forward, F, and reverse, R), and the length of the amplified products were as follows: NMHC-IIA (F: GTGCAATGATGTCCTGTT; R: CTGGTTACAGAGCAGGTG (267-bp product).

Nodal$^{\Delta 600}$ Mice

The asymmetric expression of Nodal in the left LPM is governed by the intronic enhancer (ASE) element within the first intron of Nodal that is Foxh1 dependent (Norris and Robertson, 1999; Saijoh et al., 2000). Targeted deletion of this 596-bp enhancer sequence involved homologous recombination in ES cells replacing the ASE with a lox-flanked PGK-hygromycin cassette which was subsequently excised by Cre-mediated recombination resulting in the Nodal$^{\Delta 600}$ allele. Embryos homozygous for this deletion (Nodal$^{\Delta 600/\Delta 600}$) display reduced left-sided Nodal expression, but the early events controlling left–right axis specification are correctly initiated (Norris et al., 2002). Loss of the ASE alters Lefty2 expression and results in delayed Pitx2 expression leading to late onset, left–right patterning defects (Norris et al., 2002). Nodal$^{\Delta 600/\Delta 600}$ embryos and wild-type controls from intercrosses of Nodal$^{\Delta 600}$ mice on an ICR background (Taconic) were harvested at E9.5 into cold PBS, fixed in 4% paraformaldehyde (PFA), dehydrated and rehydrated through a methanol series and processed for immunohistochemistry. Nodal$^{\Delta 600}$ mice and embryos were genotyped by PCR using allele specific primers. The presence of the wild-type ASE was analyzed using wild-type ASE forward (5′GAACCGGGCGTAAAA-TAAAACA-3′) and wild-type ASE reverse (5′-TGGCCCCAGAGGACAGAGG-3′); a 400-bp fragment shows the presence of the wild-type enhancer. Additionally, the deletion was directly analyzed using $^{\Delta}$600-5 (5′-GCTAGTGGCG CGATCGGAATGGA-3′) and $^{\Delta}$600-6 (5′-AAGGGAAGTGAACTGGAAAGGTATGT-3′): a 350-bp fragments indicates deletion of the ASE whereas a 950-bp fragment indicates the wild-type allele. All animal experimentation in the UK was done under UK Home Office authorization and regulations and fixed embryos were sent to our group for immunohistochemistry and RT-PCR analysis.

Echocardiography

The noninvasive echocardiography was carried out as described in detail in previous publications (Gui et al., 1996; Linask and Huhta, 2000). Cur-

rent instrumentation being used is the VisualSonics Vevo770 system.

ACKNOWLEGMENTS

We thank Dr. Elizabeth J. Robertson of Wellcome Trust Centre for Human Genetics for sharing the Nodal$^{\Delta 600}$ mouse model; and Dr. Robert Adelstein at NHLBI for providing us with the NMHC-IIB transgenic breeding pairs and for the NMHC-IIC antibodies. K.K.L. was funded by an Established Investigator grant from the American Heart Association and the Suncoast Cardiovascular Research and Education Foundation (funded by Helen Harper Brown).

REFERENCES

Ai D, Liu W, Ma L, Dong F, Lu MF, Wang D, Verzi MP, Cai CL, Gage PJ, Evans S, Black BL, Brown NA, Martin JF. 2006. Pitx2 regulates cardiac left-right asymmetry by patterning second cardiac lineage-derived myocardium. Dev Biol 296: 437–449.

Baldwin HS, Solursh M. 1989. Degradation of hyaluronic acid does not prevent looping of the mammalian heart in situ. Dev Biol 136:555–559.

Blake KJ, Myette G, Jack J. 1998. The products of ribbon and raw are necessary for proper cell shape and cellular localization of nonmuscle myosin in Drosophila. Dev Biol 203:177–188.

Blake KJ, Myette G, Jack J. 1999. ribbon, raw, and zipper have distinct functions in reshaping the Drosophila cytoskeleton. Dev Genes Evol 209:555–559.

Conti MA, Even-Ram S, Liu C, Yamada KM, Adelstein RS. 2004. Defects in cell adhesion and the visceral endoderm following ablation of nonmuscle myosin heavy chain II-A in mice. J Biol Chem 279:41263–41266.

Davis JS, Hassanzadeh S, Winitsky S, Lin H, Satorius C, Vemuri R, Aletras AH, Wen H, Epstein ND. 2001. The overall pattern of cardiac contraction depends on a spatial gradient of myosin regulatory light chain phosphorylation. Cell 107:631–641.

Discher DE, Janmey P, Wang YL. 2005. Tissue cells feel and respond to the stiffness of their substrate. Science 310:1139–1143.

Du A, Sanger JM, Linask KK, Sanger JW. 2003. Myofibrillogenesis in the first cardiomyocytes formed from isolated quail precardiac mesoderm. Dev Biol 257:382–394.

Engler AJ, Sen S, Sweeney HL, Discher DE. 2006. Matrix elasticity directs stem cell lineage specification. Cell 126:677–689.

Epstein ND, Davis JS. 2003. Sensing stretch is fundamental. Cell 112: 147–150.

Gobom J, Schuerenberg M, Mueller M, Theiss D, Lehrach H, Nordhoff E. 2001. Alpha-cyano-4-hydroxycinnamic acid affinity sample preparation. A protocol for MALDI-MS peptide analysis in proteomics. Anal Chem 73:434–438.

Gui YH, Linask KK, Khowsathit P, Huhta JC. 1996. Doppler echocardiography of normal and abnormal embryonic mouse heart. Pediatr Res 40:633–642.

Hamburger V, Hamilton HL. 1951. A series of normal stages in the development of the chick embryo. J Morphol 88:49–92.

Hollyfield JG. 1999. Hyaluronan and the functional organization of the interphotoreceptor matrix. Invest Ophthalmol Vis Sci 40:2767–2769.

Imanaka-Yoshida K, Knudsen K, Linask KK. 1998. Initial myofibrillogenesis in precardiac mesoderm cultures. Cell Motil Cytoskeleton 39:52–62.

Itasaki N, Nakamura H, Sumida H, Yasuda M. 1991. Actin bundles on the right side in the caudal part of the heart tube play a role in dextro-looping in the embryonic chick heart. Anat Embryol (Berl) 183:29–39.

Kang D, Gho YS, Suh M, Kang C. 2002. Highly sensitive and fast protein detection with coomassie brilliant blue in sodium dodecyl sulfate-polyacrylamide gel electrophoresis. Bull Korean Chem Soc 23:1511–1512.

Kawabata S, Usukura J, Morone N, Ito M, Iwamatsu A, Kaibuchi K, Amano M. 2004. Interaction of Rho-kinase with myosin II at stress fibres. Genes Cells 9:653–660.

Kostetskii I, Li J, Xiong Y, Zhou R, Ferrari VA, Patel VV, Molkentin JD, Radice GL. 2005. Induced deletion of the N-cadherin gene in the heart leads to dissolution of the intercalated disc structure. Circ Res 96:346–354.

Lash JW, Linask KK, Yamada KM. 1987. Synthetic peptides that mimic the adhesive recognition signal of fibronectin: differential effects on cell-cell and cell-substratum adhesion in embryonic chick cells. Dev Biol 123:411–420.

Lash JW, Rhee D, Zibrida JT, Philp N. 1992. A monoclonal antibody that reacts with the ventro-caudal quadrant of newly formed somites. In: Bellairs R, Sanders EJ, Lash JW, editors. Formation and differentiation of early embryonic mesoderm. New York: Plenum Press. p 169–180.

Latacha KS, Remond MC, Ramasubramanian A, Chen AY, Elson EL, Taber LA. 2005. Role of actin polymerization in bending of the early heart tube. Dev Dyn 233:1272–1286.

Linask KK. 1992a. N-cadherin localization in early heart development and polar expression of Na, K-ATPase, and integrin during pericardial coelom formation and epithelialization of the differentiating myocardium. Dev Biol 151:213–224.

Linask KK. 1992b. Regulatory role of cell adhesion molecules in early heart development. In: Bellairs R, Sanders EJ, Lash JW, editors. Formation and differentiation of early embryonic mesoderm. New York: Plenum Publishing Corporation. p 301–313.

Linask K. 2003. Regulation of heart morphology: current molecular and cellular perspectives on the coordinated emergence of cardiac form and function. Birth Defects Res C Embryo Today 69:14–24.

Linask KK, Huhta JC. 2000. Use of Doppler echocardiography to monitor embryonic mouse heart function. Methods Mol Biol 1:245–252.

Linask KK, Lash JW. 1986. Precardiac cell migration: fibronectin localization at mesoderm-endoderm interface during directional movement. Dev Biol 114:87–101.

Linask KK, Lash JW. 1988. A role for fibronectin in the migration of avian precardiac cells. I. Dose dependent effects of fibronectin antibody. Dev Biol 129:315–323.

Linask KK, Lash JW. 1990. Fibronectin and integrin distribution on migrating precardiac mesoderm cells. Ann N Y Acad Sci 588:417–420.

Linask KK, Lash JW. 1998. Morphoregulatory mechanisms underlying early heart development: precardiac stages to the looping, tubular heart. In: Cruz MD, Markwald R, editors. Living morphogenesis of the heart. Boston, MA: Birkhauser.

Linask KK, Tsuda T. 2000. Application of plastic embedding for sectioning whole-mount immunostained early vertebrate embryos. In: Tuan RS, Lo CW, editors. Developmental biology protocols. Totowa, NJ: Humana. p 165–173.

Linask KK, VanAuker M. 2007. A role for the cytoskeleton in heart looping. ScientificWorldJournal 7:280–298.

KK, Knudsen KA, Gui YH. 1997. N-Cadherin-catenin interaction: necessary component of cardiac cell compartmentalization during early vertebrate heart development. Dev Biol 185:148–164.

Linask KK, Yu X, Chen YP, Han MD. 2002. Directionality of heart looping: effects of Pitx2c misexpression on flectin asymmetry and midline structures. Dev Biol 246: 407–417.

Linask K, Han M, Linask K, Schlange T, Brand T. 2003a. Effects of antisense misexpression of CFC on downstream flectin protein expression during heart looping. Dev Dyn 228:217–230.

Linask KK, Han MD, Linask KL, Schlange T, Brand T. 2003b. Effects of antisense misexpression of CFC on downstream flectin protein expression during heart looping. Dev Dyn 228:217–230.

Linask KK, Han M, Cai DH, Brauer PR, Manisastry SM. 2005a. Cardiac morphogenesis: matrix metalloproteinase coordination of cellular mechanisms underlying heart tube formation and directionality of heart looping. Dev Dyn 233:739–753.

Linask KK, Manisastry SM, Han M. 2005b. Cross-talk between cell-cell and cell-matrix adhesion signaling pathways during heart organogenesis: implication for cardiac birth defects. Microsc Microanal 11:200–208.

Manasek FJ. 1976a. Glycoprotein synthesis and tissue interactions during establishment of the functional embryonic chick heart. J Mol Cell Cardiol 8:389–402.

Manasek FJ. 1976b. Heart development: interactions involved in cardiac morphogenesis. In: Poste G, Nicolson GL, editors. The cell surface in animal embryogenesis and development. Amsterdam: Elsevier/North-Holland Biomedical Press. p 545–598.

Manasek FJ, Burnside MB, Waterman RE. 1972. Myocardial cell shape change as a mechanism of embryonic looping. Dev Biol 29:349–371.

Marigo V, Nigro A, Pecci A, Montanaro D, Di Stazio M, Balduini CL, Savoia A. 2004. Correlation between the clinical phenotype of MYH9-related disease and tissue distribution of class II nonmuscle myosin heavy chains. Genomics 83:1125–1133.

Meshel AS, Wei Q, Adelstein RS, Sheetz MP. 2005. Basic mechanism of three-dimensional collagen fibre transport by fibroblasts. Nat Cell Biol 7:157–164.

Mieziewska K, Szel A, Van Veen T, Aguirre GD, Philp N. 1994. Redistribution of insoluble interphotoreceptor matrix components during photoreceptor differentiation in the mouse retina. J Comp Neurol 345:115–124.

Norris DP, Robertson EJ. 1999. Asymmetric and node-specific nodal expression patterns are controlled by two distinct cis-acting regulatory elements. Genes Dev 13:1575–1588.

Norris DP, Brennan J, Bikoff EK, Robertson EJ. 2002. The Foxh1-dependent autoregulatory enhancer controls the level of Nodal signals in the mouse embryo. Development 129:3455–3466.

Perkins DN, Pappin DJ, Creasy DM, Cottrell JS. 1999. Probability-based protein identification by searching sequence databases using mass spectrometry data. Electrophoresis 20:3551–3567.

Pollard TD. 2003. The cytoskeleton, cellular motility and the reductionist agenda. Nature 422:741–745.

Price RL, Chintanowonges C, Shiraishi I, Borg TK, Terracio L. 1996. Local and regional variations in myofibrillar patterns in looping rat hearts. Anat Rec 245: 83–93.

Saijoh Y, Adachi H, Sakuma R, Yeo CY, Yashiro K, Watanabe M, Hashiguchi H, Mochida K, Ohishi S, Kawabata M, Miyazono K, Whitman M, Hamada H. 2000. Left-right asymmetric expression of lefty2 and nodal is induced by a signaling pathway that includes the transcription factor FAST2. Mol Cell 5:35–47.

Schuerenberg M, Luebbert C, Eickhoff H, Kalkum M, Lehrach H, Nordhoff E. 2000. Prestructured MALDI-MS sample supports. Anal Chem 72:3436–3442.

Shevchenko A, Wilm M, Vorm O, Mann M. 1996. Mass spectrometric sequencing of proteins silver-stained polyacrylamide gels. Anal Chem 68:850–858.

Shiraishi I, Takamatsu T, Minamikawa T, Fujita S. 1992. 3-D observation of actin filaments during cardiac myofibrillogenesis in chick embryo using a confocal laser scanning microscope. Anat Embryol (Berl) 185:401–408.

Shiraishi I, Takamatsu T, Fujita S. 1993. 3-D observation of N-cadherin expression during cardiac myofibrillogenesis of the chick embryo using a confocal laser scanning microscope. Anat Embryol (Berl) 187:115–120.

Shiraishi I, Takamatsu T, Fujita S. 1995. Three-dimensional observation with a confocl scanning laser microscope of fibronectin immunolabeling during cardiac looping in the chick embryo. Anat Embryol (Berl) 191:183–189.

Shiraishi M, Wang X, Walsh MP, Kargacin G, Loutzenhiser K, Loutzenhiser R. 2003. Myosin heavy chain expression in renal afferent and efferent arterioles: relationship to contractile kinetics and function. FASEB J 17:2284–2286.

Speder P, Adam G, Noselli S. 2006. Type ID unconventional myosin controls left-right asymmetry in Drosophila. Nature 440:803–807.

Spodik B, Seeholzer SH, Coleman C. 2002. In: Coleman EA, editor. Protein-protein interactions. Cold Spring Harbor, NY: Cold Spring Harbor Laboratory Press. p 355–374.

Sumida H, Ashcraft RA Jr, Thompson RP. 1989. Cytoplasmic stress fibers in the developing heart. Anat Rec 223:82–29.

Tsuda T, Philp N, Zile MH, Linask KK. 1996. Left-right asymmetric localization of flectin in the extracellular matrix during heart looping. Dev Biol 173:39–50.

Tsuda T, Majumder K, Linask KK. 1998. Differential expression of flectin in the extracellular matrix and left-right asymmetry in mouse embryonic heart during looping stages. Dev Genet 23:203–214.

Tullio AN, Accili D, Ferrans VJ, Yu ZX, Takeda K, Grinberg A, Westphal H, Preston YA, Adelstein RS. 1997. Nonmuscle myosin II-B is required for normal development of the mouse heart. Proc Natl Acad Sci U S A 94: 12407–12412.

Vemuri R, Lankford EB, Poetter K, Hassanzadeh S, Takeda K, Yu ZX, Ferrans VJ, Epstein ND. 1999. The stretch-activation response may be critical to the proper functioning of the mammalian heart. Proc Natl Acad Sci U S A 96:1048–1053.

Wei L, Roberts W, Wang L, Yamada M, Zhang S, Zhao Z, Rivkees SA, Schwartz RJ, Imanaka-Yoshida K. 2001. Rho kinases play an obligatory role in vertebrate embryonic organogenesis. Development 128:2953–2962.

Wei L, Imanaka-Yoshida K, Wang L, Zhan S, Schneider MD, DeMayo FJ, Schwartz RJ. 2002. Inhibition of Rho family GTPases by Rho GDP dissociation inhibitor disrupts cardiac morphogenesis and inhibits cardiomyocyte proliferation. Development 129:1705–1714.

Yost HJ. 1992. Regulation of vertebrate left-right asymmetries by extracellular matrix. Nature 357:158–161.

Developmental Dynamics